第 26 卷第 4 期 无 机 化 学 学 报 Vol.26 No.4
2010 年 4 月 CHINESE JOURNAL OF INORGANIC CHEMISTRY 567-572

用 MnO_2 离子筛吸附剂从溶液中提取锂

孙淑英 张钦辉 于建国*
(华东理工大学化学工程联合国家重点实验室,上海 200237)

摘要: 研究了 MnO_2 离子筛的制备、表征及其提锂性能。通过控制低温水热合成反应条件制备了 4 种不同晶相的一维纳米 MnO_2,进一步用浸渍法制备了 Li-Mn-O 三元氧化物前驱体,并经酸处理后得到对 Li^+具有特殊选择性的离子筛。用 XRD、吸附等温线、吸附动力学及 pH 滴定等手段对产物的晶相结构和 Li^+吸附性能进行了研究。结果表明,SMO-b 和 SMO-d 离子筛的 Li^+平衡吸附量符合 Freundlich 吸附等温方程。反应物浓度对 MnO_2 不同晶面的生长速率有不同的影响,但$(NH_4)_2SO_4$ 对吸附容量并无提高。吸附速率方程符合一级动力学 Lagergren 方程。MnO_2 离子筛 Li^+的吸附量远远高于 Na^+。

关键词: 锂; 吸附等温线; 卤水; 离子筛吸附剂; MnO_2
中图分类号: O614.71+1; O614.111; TQ028.15; TQ424.2 **文献标识码**: A **文章编号**: 1001-4861(2010)04-0567-06

MnO_2 Ion Sieve Adsorbent for Recovering Lithium from Solutions

SUN Shu-Ying ZHANG Qin-Hui YU Jian-Guo*
(*State Key Lab of Chemical Engineering, East China University of Science and Technology, Shanghai* 200237)

Abstract: The paper presents preparation and characterization of the MnO_2 ion sieve for recovering lithium from aqueous media. Different MnO_2 polymorphs, produced by low temperature hydrothermal oxidation of Mn^{2+} by $S_2O_8^{2-}$ with or without $(NH_4)_2SO_4$ at 393 and 423 K, were employed to prepare 4 MnO_2 based ion sieve adsorbents. The structure characteristics, adsorption and ion-exchange properties of the adsorbent were studied by XRD analysis and experimental runs for the Li^+ isotherms, adsorption kinetic data and the effect of initial pH value on the capacity. The capacities of SMO-b and SMO-d adsorbents for Li^+ vs. its equilibrium concentration data were well fitted by the Freundlich adsorption isotherm model. The relative capacity data suggest that $(NH_4)_2SO_4$ is not necessary for the oxidation. The first order reaction kinetics model is adequate to predict the Li^+ concentration decay curves of the kinetic runs. The MnO_2 based ion sieve adsorbent exhibits an order of magnitude higher capacity for Li^+ than for Na^+.

Key words: aqueous resources of lithium; adsorption isotherm; brine; ion-sieve adsorbent; MnO_2

0 Introduction

Lithium is the lightest metal and is highly reactive in the elemental form, therefore, it exists in the nature primarily as spodumene in minerals and/or lithium ions (Li^+) in brine and seawater. Lithium compounds, such as LiCl, Li_2CO_3 and $LiOH \cdot H_2O$ are often employed for making ceramics and glass, aluminum production,

收稿日期:2009-12-10。收修改稿日期:2010-03-02。
国家自然科学基金(No.20906022),上海市科委纳米专项基金(No.0852nm021)资助项目。
*通讯联系人。E-mail:jgyu@ecust.edu.cn
第一作者:孙淑英,女,31 岁,博士,讲师;研究方向:无机氧化物的制备及应用。

pharmaceuticals, and batteries as well as for thermonuclear power generation, military and many other applications[1-3]. The worldwide lithium consumption has increased rapidly from less than 100 tons per year of lithium carbonate equivalent in the early 1 900 s to more than 70 000 tons per year one hundred years later[4]. Production of lithium carbonate from minerals is energy intensive, environmentally unsound and is capacity limited due to the shortage of high grade Li containing minerals. Sustainable development of the lithium industry in China will depend on cost effective large scale utilization of its salt lake brine resources which accounts for 80% of the national lithium reserves.

Lithium from brine or seawater can be recovered by solvent extraction[5], precipitation and adsorption[6-7]. Solvent extraction is the least attractive one since the high cost of organic solvent and its potential hazard in large scale operation. Precipitation technology has been successfully employed for commercial production of Li compounds where salt lake brine with a high Li content and low molar ratio of Mg/Li is readily available. It is not cost effective for Li recovery from brine with a low Li content and/or with a n_{Mg}/n_{Li}>1400, such as the case for most salt lakes in China and Dead Sea of Jordan[8]. Adsorption process employing a highly selective ion sieve adsorbent is the most attractive technology for Li recovery from low-grade brine or seawater because it is both cost effective and environmental friendly since its high capacity for Li^+ may be regenerated for multi-cycle operations.

MnO_2 and TiO_2 are known to have high adsorptive capacity for Li^+ [9-11]. However, there have been no systematic studies on the effect of different polymorphs of MnO_2 precursor on the Li^+ extraction process. In this work, several polymorphs of MnO_2 produced by a hydrothermal method were employed to prepare the MnO_2 based ion sieve adsorbent. The structure characteristics and ion-exchange property of the adsorbent were studied by XRD, pH titration, equilibrium capacity and kinetic experiments. The experimental data are reviewed for potential application for recovering Li from brine or seawater.

1 Experimental

1.1 Preparation of MnO_2 based ion sieve adsorbent

To prepare the Li-Mn-O precursor, different polymorphic forms of MnO_2 were first produced by controlled low-temperature hydrothermal oxidation of Mn^{2+} by $S_2O_8^{2-}$:

$$MnSO_4+(NH_4)_2S_2O_8+2H_2O \rightarrow MnO_2+(NH_4)_2SO_4+2H_2SO_4 \quad \Delta G^{\ominus} = -151\ kJ\cdot mol^{-1} \qquad (1)$$

The reaction is thermodynamically favored as suggested by its highly negative change of the standard Gibbs free energy.

Analytical grade $MnSO_4\cdot H_2O$ (0.25 mol) and the stoichiometric amount of $(NH_4)_2S_2O_8$ (0.25 mol) were added to 750 mL of deionized water to form a homogeneous solution at the room temperature, transferred to a stainless steel autoclave, then sealed and maintained for 12 h at 393 K(for MO-a) and 423 K (for MO-b), respectively. The resulting black solid products were filtered, washed completely with deionized water to remove residual free ions in the final products and finally dried at 393 K for 8 h in static air to result in MO-a and MO-b. MO-c and MO-d were produced in the same manner except that 0.47 mol of analytical grade $(NH_4)_2SO_4$ was included as the extra reactant.

Four Li-Mn-O precursors (LMO-a, -b, -c, -d) were prepared by wet impregnation of Li on MO-a, -b, -c, -d. Mixtures of the MO particles and aqueous solution of LiOH (0.35 $mol\cdot L^{-1}$, n_{Li}/n_{Mn}=0.55) were heated in a rotary evaporator at 393 K for 12 h to remove water and then calcined at 1 003 K for 6 h in static air. Acid treatment was performed then to remove Li^+ from the Li-Mn-O precursors; 4 g of LMO-a, -b, -c, -d were each contacted with a hydrochloric acid(200 mL, 0.5 $mol\cdot L^{-1}$) for 120 h, till the Li^+ were extracted completely from the Li-Mn-O lattice, as measured by Metrohm 861 IC with Metrosep C2 100/4.0 column. The acid-treated materials were filtered, washed with deionized water, and dried at 393 K for 8 h to obtain MnO_2 ion sieve adsorbents (SMO-a, -b, -c, -d). Fig.1 presents the flow diagram of the procedures employed for preparation of the MnO_2 ion sieve adsorbents.

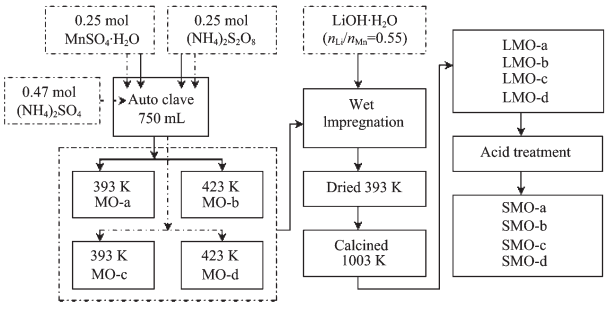

Fig.1　Flow diagram of the procedures for preparation of the MnO_2 ion sieve adsorbents

1.2　Characterization of the MnO_2 adsorbent

1.2.1　Structural characterization

Phase purity of the samples was examined by X-ray diffraction (XRD) analysis using a Rigaku D/max 2550 X-ray diffractometer with Cu $K\alpha$ radiation (λ = 0.154 056 nm), operating at 40 kV, 100 mA and scanning rate of $10°\cdot min^{-1}$.

1.2.2　Adsorption equilibrium capacity and kinetic experiments

In the adsorption equilibrium capacity test run, 0.10 g of MnO_2 ion sieve adsorbent was introduced to a series of 100 mL of LiCl solutions of different initial concentrations (1.99, 4.05, 6.09, 8.12, 10.10, 12.31, 16.41, 20.37, 24.73, 30.24, 51.12 $mmol\cdot L^{-1}$) at a pH value of 10.1 maintained by a buffer solution(0.10 $mol\cdot L^{-1}$ NH_4Cl and 0.10 $mol\cdot L^{-1}$ NH_4OH), under stirring (130 $r\cdot min^{-1}$) for 144 h at 303 K. The final (equilibrium) concentration of Li^+ of the supernatant was measured *in-situ* by IC. In the adsorption rate test run, 0.10 g of MnO_2 was introduced to a series of 100 mL LiCl solutions (10.19 $mmol\cdot L^{-1}$, pH=10.1) under stirring(130 $r\cdot min^{-1}$) at 303 K; One of the samples was taken periodically for measurement of Li^+ of the supernatant until its concentration was nearly constant.

The exchange capacity or the amount of lithium ion adsorbed per gram of MnO_2 was calculated according to equation (**2**):

$$Q = (C_0 - C)\cdot V/W \qquad (2)$$

where: Q-amount of Li^+ adsorbed per gram of adsorbent ($mmol\cdot g^{-1}$); C-Li^+ concentration ($mol\cdot L^{-1}$); C_0- initial Li^+ concentration($mol\cdot L^{-1}$); V-sample volume (100 mL); W-weight of adsorbent(0.1 g).

1.2.3　Effect of initial pH value on the adsorbents capacity for Li^+ and Na^+

0.10 g of MnO_2 was added to 10 mL of mixture of 0.10 $mol\cdot L^{-1}$ MeCl and MeOH in various ratios(Me=Li and Na) under stirring(130 $r\cdot min^{-1}$) for 144 h at 303 K. The Li^+ concentration of the supernatant solution was measured by IC, and the final pH value of the solution was measured using Metrohm 827 pH Lab Meter with Pt 1000 electrode.

2　Results and discussion

2.1　Structural characterization

The XRD patterns in Fig.2-A shows that the reflections of MO-a and -b are indexed to a mixture of orthorhombic phase of ramsdellite-MnO_2(PDF 39-0375, with lattice constants a=0.927 0 nm, b=0.286 6 nm, c=0.453 3 nm) and tetragonal phase of α-MnO_2 with(PDF 44-0141, a=0.978 5 nm, c=0.286 3 nm) and that those of MO-c and d are pure tetragonal phase of α-MnO_2 (PDF 44-0141) with a faint diffraction peak at 22.36° associated with trace amount of orthorhombic MnO_2. Thus pure α-MnO_2 may be obtained by proper control of the hydrothermal oxidation conditions. Tetragonal MnO_2 is constructed from double chains of [MnO_6] octahedral

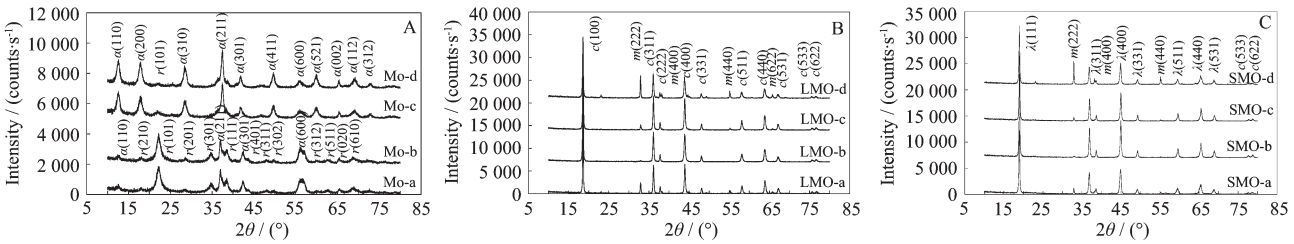

$\alpha(hkl)$: α-MnO_2 crystal face; $r(hkl)$: ramsdellite MnO_2 crystal face; $c(hkl)$: cubic $LiMn_2O_4$ crystal face; $m(hkl)$: cubic Mn_2O_3 crystal face; $\lambda(hkl)$: cubic MnO_2 crystal face

Fig.2　XRD patterns-A: the oxidation products, B: Li-Mn-O precursors, C: MnO_2 adsorbents.

unit forming 2×2 tunnels. NH_4^+ and SO_4^{2-} coexist with Mn^{2+} and $S_2O_8^{2-}$ in both reaction systems, thus affecting the crystal structure and morphology of the products. Higher SO_4^{2-} results in a lower formation rate of Mn^{4+} and thus the lower formation rate of various crystal faces of tetragonal-MnO_2. The reactant composition affects the formation rate of different crystal forms resulting in various crystal MnO_2 structures.

As the reaction temperature is increased from 393 K to 423 K, there is no transformation of crystal structure, as illustrated in the XRD patterns for MO-a/-b vs. MO-c/-d. Further study is in progress to determine the relative importance of the temperature and the reactant composition on the adsorbent structure.

The reflection peaks in Fig.2-B are much slimmer and sharper relative to those in Fig.2-A due to smaller crystalline dimension. Almost all the reflections in Fig. 2-B are indexed to cubic phase of $LiMn_2O_4$ (PDF 35-0782, lattice constant=0.824 8 nm). The several faint diffraction peaks (33.04°, 38.36°, 55.54° and 66.22°) are associated with trace amounts of cubic phase of Mn_2O_3 crystal face (PDF 41-1442. lattice constant a= 0.940 9 nm) produced at a relatively low calcination temperature[12].

The reflections in Fig.2-C are denoted as pure cubic phase of λ-MnO_2(PDF 44-0992, lattice constant= 0.803 0 nm). Several faint diffraction peaks at 32.96°, 55.32°, 77.92° and 78.92 are likely due to trace amounts of cubic Mn_2O_3 and cubic $LiMn_2O_4$ produced by the residual Li^+ on the surface. The similar XRD patterns shown in Fig.2-B and 2-C demonstrate that the Li-Mn-O precursors and the corresponding MnO_2 adsorbents are both cubic phase crystals with slightly different lattice constants. Although the Li^+ inserted in the Mn-O lattice will result in larger lattice dimension, the Li-Mn-O precursor is very stable during the Li^+ extraction process that the Mn sites of the crystal structure are well maintained.

2.2 Adsorption equilibrium capacity and kinetic experiments

Fig.3-A shows the Li^+ adsorption isotherm of MnO_2 ion-sieve. According to Freundlich adsorption isotherm as shows in equation (**3**), the adsorption data are further simulated as in Fig.3-B.

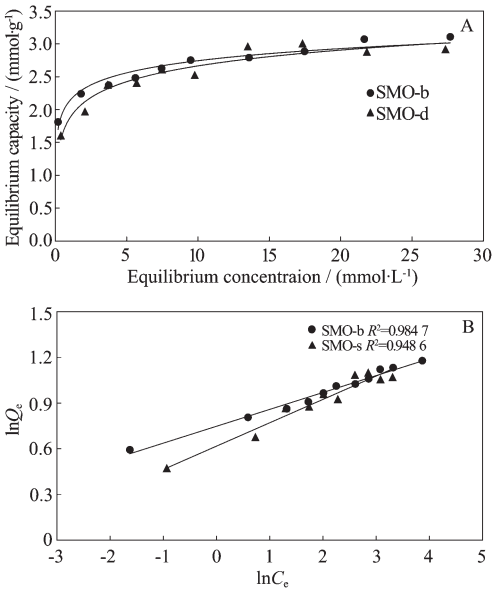

T=303 K; pH=10.1; V=100 mL; W=0.10 g; contact time=120 h

Fig.3 Li^+ adsorption isotherms of MnO_2 ion-sieves adsorbents (A) and simulated according to Freundlich equation (B)

$$\ln Q_e = 1/n \cdot \ln C_e + \ln K_f \quad (3)$$

Q_e is amount of lithium ion adsorbed per gram of adsorbent at equilibrium (mmol·g^{-1}); C_e, equilibrium concentration of lithium ions(mol·L^{-1}); n and K_f, Freundlich constants. As shown in Fig.3-A, the exchange capacity of SMO-b is larger than that of SMO-d in low concentration of Li^+ solution, but there is no difference as the initial concentration of lithium ions exceeds 0.02 mol·L^{-1}. It is possible that relatively higher purity of SMO-b, resulted from the higher purity of LMO-b precursor, has higher Li^+ adsorption capacity at low Li^+ concentration. It is apparent that the data present quite good linearity in Fig.3-B, indicating that the lithium ion exchange process in the experiment is well accorded with the Freundlich adsorption isotherm.The adsorption constant of SMO-b and SMO-d is calculated to be n=9.03, K_f=4.54, and n=6.51, K_f= 5.35, respectively, which shows the adsorption is easy to process.

Fig.4-A shows the lithium adsorption kinetics of MnO_2 ion-sieves under certain reaction conditions. The adsorption kinetics is examined with a first-order rate expression, the so-called Lagergren equation (**4**)[13], as in

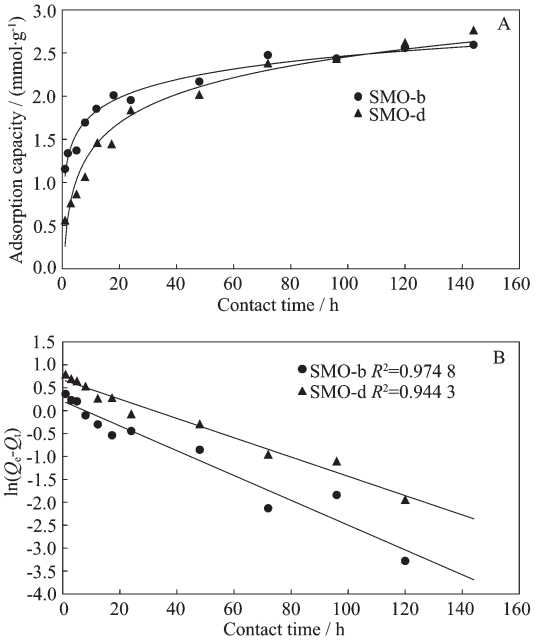

T=303 K; pH=10.1; *V*=100 mL; *W*=0.10 g

Fig.4　Li^+ adsorption kinetics of MnO_2 ion-sieves adsorbents (A) and simulated according to Lagergren equation (B)

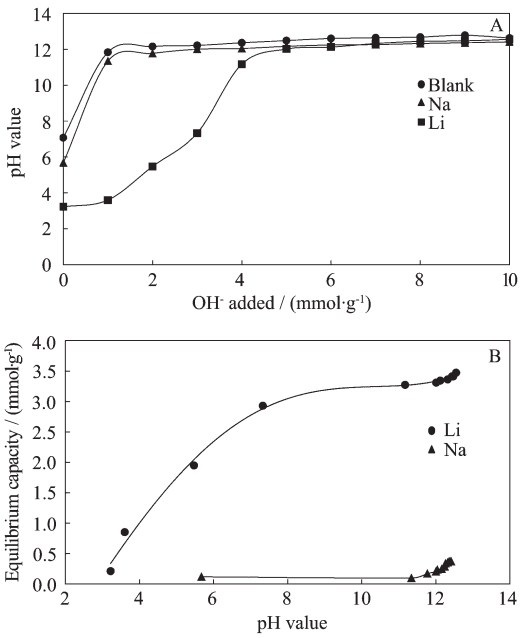

T=303 K; pH=10.1; *V*=10 mL(0.1 mol·L^{-1} MeCl+MeOH; Me= Li^+ and Na^+); *W*=0.10 g; contact time=144 h

Fig.5　pH titration curves (A) and adsorption capacity (B) toward lithium and sodium ions of ion-sieve at different pH values

Fig.4-B.

$$\ln(Q_e - Q_t) = \ln Q_e - k_{ads} \cdot t \quad (4)$$

Q_t is amount of lithium ion adsorbed per gram of adsorbent at time t (mmol·g^{-1}); k_{ads}, adsorption rate constant(s^{-1}); t, contact time(s)

As shown in Fig.4-A, the adsorption rate of SMO-b is faster than that of SMO-d before 96 h, and there is no difference after. It also shows that adsorption of Li^+ on SMO-b is easier than that on SMO-d, indicating that the ternary Li-Mn-O precursor has great influence on the Li^+ adsorptive property of the final Mn-O ion-sieve. Fig.4-B shows reasonably good linearity on the plot of $\ln(Q_e - Q_t)$, showing that the adsorption rate can be well described by first-order kinetics before attaining equilibrium. The value of the adsorption rate constant is calculated, via the linear slope, to be 7.53×10^{-6} and 5.83×10^{-6} s^{-1}, respectively, indicating a rather slow adsorption rate, which is probably resulted from the current static adsorption condition.

2.3　Effect of initial pH value on the adsorbents capacity for Li^+ and Na^+

The pH titration curves and adsorption capacity of SMO-b ion sieve toward lithium and sodium ions are shown in Fig.5-A and -B, respectively. The titration curve shows monacid behavior with a high exchange capacity for lithium ions, yet pretty low exchange capacities for sodium ions over the pH range studied. The ion-exchange capacity reaches 3.47 mmol·g^{-1} for lithium ions and only 0.37 mmol·g^{-1} for sodium ions at pH value of 12.5, indicating that the sample exhibits a remarkable lithium ion-sieve property. The high selectivity for Li^+ is due to the steric effect of the insertion site. And the Na^+ uptake can be regarded as the number of nonspecific ion-exchange sites on the surfaces of the powder [14]. SMO-b ion sieve shows a dibasic acid behavior. A stronger acidic site, dissociating below pH value of 4, can be ascribed to Li^+-specific ion-exchange sites, and weaker acidic sites, dissociating above pH value of 4, can be ascribed to redox-type sites.

3　Conclusions

(1) Four MnO_2 polymorphs were produced by low temperature hydrothermal oxidation of oxidation of Mn^{2+} by $S_2O_8^{2-}$ with and without $(NH_4)_2SO_4$ at 393 and 423 K.

The different MnO_2 polymorphs were employed to prepare 4 MnO_2 based ion sieve adsorbents with different structural and adsorptive properties.

(2) The $LiMn_2O_4$ precursor is very stable during the Li^+ extraction process and that the locations of Mn in the crystal structure are well maintained.

(3) Adsorptive capacities of SMO-b and SMO-d adsorbents for Li^+ are well represented by the Freundlich adsorption model. The generally higher relative capacities of SMO-b suggest that addition of $(NH_4)_2SO_4$ is not necessary.

(4) The adsorption kinetic data are consistent with the apparent first order reaction kinetics.

(5) The highly selective nature of the experimental adsorbent is demonstrated by its much higher capacity for Li^+ and Na^+, and the capacities for both increase with a higher initial pH value employed in the test run.

References:

[1] Ammundsen B, Paulsen J. *Adv. Mater.*, **2001**,**13**(12/13):943-956

[2] Shaju K M, BruceA P G. *Chem. Mater.*, **2008**,**20**(17):5557-5562

[3] Wen X M, Ma P H, Zhu C L, et al. *Sep. Purif. Technol.*, **2006**,**49**(3):230-236

[4] Ebensperge A, Maxwell P, Moscoso C. *Resources Policy*, **2005**,**30**(3):218-231

[5] Bukowsky H, Uhlemann E, Gloe K, et al. *Hydrometallurgy*, **1992**,**28**(3):323-329

[6] Koyanaka H, Matsubaya O, Hatta N. *J. Electroanal. Chem.*, **2003**,**559**:77-81

[7] Chitrakar R, Kanoh H, Miyai Y, et al. *Chem. Mater.*, **2000**, **12**(10):3151-3157

[8] Zhang Q H, Sun S Y, Li S P, et al. *Chem. Eng. Sci.*, **2007**, **62**(18/19/20):4869-4874

[9] Feng Q, Miyai Y, Kanoh H, et al. *Langmuir*, **1992**,**8**(7):1861-1867

[10]Feng Q, Kanoh H, Ooi K. *J. Mater. Chem.*, **1999**,**9**(2):319-333

[11]LI Shao-Peng(李少鹏), ZHANG Qin-Hui(张钦辉), SUN Shu-Ying(孙淑英), et al. *J. Tianjin Univ.*(*Tianjin Daxue Xuebao*), **2007**,**4**:453-456

[12]Hwang B J, Santhanam R, Liu D G. *J. Power Source*, **2001**, **97**:443-446

[13]Trivedi H C, Patel V M. *Eur. Polymer J.*, **1973**,**9**:525-531

[14]Ooi K, Miyai Y, Sakakihara J. *Langmuir*, **1991**,**7**(6):1167-1171